Study of Hydraulic Tunnels in Rock Masses – Caniçada Dam

Paulo Sérgio Furtado Mendes Serafim da Cruz Antão Alves
paulo.alves@tecnico.ulisboa.pt

Instituto Superior Técnico, Lisboa, Portugal

May 2017

Abstract

The revision of the Portuguese Dams Security Regulation fostered the improvement of Caniçada Dam's discharge capacity and an auxiliary spillway was designed.

For safety reasons, a temporary rock plug was left unexcavated upstream and it is a common practice to adopt a thickness equivalent to 2-3 tunnel diameters for these temporary structures. In this case a thickness of 27.5 metres was adopted. As this feature is removed when the construction of the spillway is nearly finished, its excavation is time-consuming and can extend the works for about 2-3 months.

The objective of this work was to perform a numerical analysis of the construction of the spillway to determine the minimum thickness of the rock plug that could endure a water-induced pressure in an emergency scenario. Additionally, a parametric analysis was undertaken to evaluate the influence of relevant parameters over the thickness. It was found that for the worst scenario considered, the minimum thickness was 12 metres, less than 50% of the adopted dimension, suggesting that the allocation of resources could have been reduced, to some extent. The results obtained show some evidence that the traditional method of considering 2-3 tunnel diameters for this thickness might be too conservative for similar geological scenarios.

Lastly, a stability analysis was carried out in order to understand the failure mechanisms inside the tunnel shaft and evaluate the primary support solution of the tunnel. It was concluded that the support solution adopted in the construction works was suitable for the discontinuities set considered.

Keywords: hydraulic tunnel, rock plug, numerical analysis, finite element method, stability analysis, rock mechanics

1 Introduction

The revision of the Portuguese Dams Security Regulation fostered several projects regarding the improvement of the discharge capacity of dams. These projects are frequently related to the construction of new hydraulic features, such as auxiliary spillways. This was the case of Caniçada Dam, where the discharge capacity had to be increased and a new spillway was designed.

During the construction of the spillway, a temporary safety rock plug was left unexcavated on the upstream section as a safety measure for an emergency scenario. It is a common practice to adopt a thickness equivalent to two or three tunnel diameters for these structures. In this case a thickness of 27.5 metres was adopted. Since this feature is only removed when the the spillway is nearly completed, its excavation can extend the works for about 2 to 3 months.

The main goal of this work was to perform a numerical analysis of the construction of the spillway to determine the minimum thickness of the rock plug that could endure a water-induced pressure in an emergency scenario. Two failure emergency scenarios were studied, the stress and deformation paths were studied and the conditions under which failure occurs and on what parameters does it depend were also assessed.

Finally, a stability analysis was carried out to understand the failure mechanisms inside the tunnel shaft and evaluate the primary support solution of the tunnel.

2 Rock masses

2.1 Introduction

During the preliminary design stages of a project, it is usual to have little information available on the geotechnical characteristics, such as shear strength resistance parameters, deformations properties, in-situ stresses and hydrologic characteristics. When ground conditions are mainly controlled by rock masses, the presence of discontinuities is also a major concern and the determination of the global mechanical properties of discontinuous rock masses can be very challenging.

2.2 Material behaviour models

As elastic-plastic mechanisms may occur in rocks under suitable environmental conditions, it seems reasonable to attempt to use plasticity theory to develop yield criteria for rocks, which is the most widely used mechanism for rock mass characterisation.

2.3 Geomechanics classifications

Since detailed information on the rock mass and its characteristics can be limited during the early stages of a project, estimation of rock parameters can be a

difficult task. To overcome this barrier, rock mass classification systems were developed.

For the purpose of this dissertation, the Rock Mass Rating classification system and the Geological Strength Index will be described in the following sections.

2.3.1 Rock Mass Rating (RMR)

The Rock Mass Rating (RMR) classification system intended to give an indicative index of the quality of a rock mass for tunnel design purposes, so that some recommendations for tunnel's support could be proposed based on past experience. To apply the RMR classification the following parameters has to be assessed for each structural region: Uniaxial compressive strength of rock material, Rock Quality Designation (RQD), Spacing of discontinuities, Condition of discontinuities, Groundwater conditions and Orientation of discontinuities.

Each of these parameters is assigned a rating and the overall RMR rating is the sum these values. The RMR rating is scaled from 0 to 100 corresponding to "very poor rock" and "very good rock", respectively.

2.3.2 The Geological Strength Index (GSI)

The Geological Strength Index (GSI) was introduced and developed to overcome some of the deficiencies that had been identified in using the RMR classification with this rock mass strength criterion [1]. As RMR is a design method based on experience, factors such as the orientation of joints are not taken into account and so it is not suitable for very poor quality rock masses [2].

The GSI was developed for application on discontinuous or jointed rock masses, in order to consider the influence of these discontinuities on its strength and deformability. The GSI rates rock masses on a scale from 0 to 100 as the rock mass strength is lower or higher and it considers the interlocking of rock pieces (blockiness) and the surface quality of discontinuities. This classification may be estimated from visual exposures or borehole cores of the rock mass.

2.4 Failure criteria

2.4.1 Mohr-Coulomb criterion

In 1776, Coulomb postulated that the shear strengths of rock and of soils are composed by two components: a constant cohesion and a normal stress-dependent frictional component.

$$\tau = c' + \sigma'_n tan\phi' \tag{1}$$

where c' is the cohesion, ϕ' is the internal friction angle and σ'_n is the effective normal stress.

Mohr-Coulomb's criterion can provide good results for continuous media, with planar discontinuities. However, it's linearity does not describe experimental peak strength envelopes in rock masses, that are generally non-linear.

2.4.2 Generalised Hoek-Brown criterion

Hoek and Brown (1980) proposed a method for obtaining estimates of the strength of heavily jointed rock masses, based upon an assessment of the interlocking of rock blocks and the condition of the surfaces between these blocks.

The original Hoek-Brown failure criterion is defined by:

$$\sigma'_1 = \sigma'_3 + \sigma_{ci}\left(m\frac{\sigma'_3}{\sigma_{ci}} + s\right)^{0.5} \tag{2}$$

where σ'_1 and σ'_3 are the principal stresses at failure, m and s are material constants which depend upon the rock mass characteristics, and σ_{ci} is the uniaxial compressive strength of the intact rock.

Then, in 1994, the Generalised Hoek-Brown criterion was introduced, incorporating the GSI.

The Generalised Hoek-Brown criterion is as follows:

$$\sigma'_1 = \sigma'_3 + \sigma_{ci}\left(m_b\frac{\sigma'_3}{\sigma_{ci}} + s\right)^{a} \tag{3}$$

where m_b is the value of the Hoek-Brown constant m for the rock mass, and s and a are constants which depend upon the rock mass characteristics.

The Hoek-Brown failure criterion should only be applied to isotropic rock masses with isotropic rock mass behaviour, in which there is a sufficient number of closely spaced discontinuities, with similar surface characteristics, that isotropic behaviour involving failure on discontinuities can be assumed.

2.4.3 Hoek-Brown equivalent Mohr-Coulomb parameters

Although the most developed empirical approach to rock masses is that introduced by Hoek and Brown, most geotechnical software do not include this failure criterion. For this reason, it is useful to represent Hoek-Brown criterion in shear stress-effective normal stress terms. The resulting shear strength envelope is non-linear and so equivalent shear strength parameters have to be determined for a given normal stress or for a small range of those stresses.

This can be done by adjusting the Hoek-Brown non-linear plot (in terms of shear stress and effective normal stress) with the Mohr-Coulomb plot for a range of minor principal stress values defined by $\sigma_t < \sigma'_3 < \sigma'_{3max}$.

The equivalent ϕ' and c' can be calculated through equations 4 and 5.

$$\phi' = sin^{-1}\left[\frac{6am_b\left(s + m_b\sigma'_{3n}\right)^{a-1}}{2(1+a)(2+a) + 6am_b\left(s + m_b\sigma'_{3n}\right)^{a-1}}\right] \tag{4}$$

$$c' = \frac{\sigma_{ci}\left[(1+2a)s + (1-a)m_b\sigma'_{3n}\right]\left(s + m_b\sigma'_{3n}\right)^{a-1}}{(1+a)(2+a)\sqrt{1 + \frac{6am_b\left(s + m_b\sigma'_{3n}\right)^{a-1}}{(1+a)(2+a)}}} \tag{5}$$

where $\sigma'_{3n} = \dfrac{\sigma'_{3max}}{\sigma_{ci}}$.

The values of c' and ϕ' obtained from this analysis are very sensitive to the range of values of the minor principal stress defined by σ'_{3max}, the upper limit of

confining stress over which the relationship between the Mohr-Coulomb and the Hoek-Brown criteria is considered.

3 Tunnels in rock masses

Tunneling and mining are probably the most overwhelming projects in geotechnical engineering. Defining the properties of the ground is a difficult task and for this reason, the geotechnical engineer needs to estimate the behaviour of the tunnel under several anticipated excavation scenarios.

3.1 Failure modes in tunnels

Knowing which failure mode to expect allows the support components to be designed efficiently to endure the instability mechanism. Failure modes can be anticipated by taking into account the following excavation instability mechanisms.

Shear failure

This failure mode consists in a squeezing action, related to time-dependent shearing, that generates a plastic zone on the outline of the tunnel.

Brittle rock failure

This type of failure occurs on highly stressed massive hard rocks with elastic-brittle behaviour and it is characterised by the generation of spalling or, in worst scenarios, rockburst events.

Wedge instability

A wedge instability occurs in low in-situ stress conditions and it depends exclusively on the structural features traced by the intersection of discontinuities such as faults or joints.

3.2 Tunnel support design

The RMR was published, Bieniawski (1989) also proposed a set of guidelines for excavation and support of rock tunnels for each of the rock mass classes defined by RMR. These guidelines provide recommendations regarding stand-up time of unsupported excavations, excavation sequence, rock bolts, shotcrete and steel sets for each of the classes of RMR values.

4 Case-study: Hydraulic tunnel in Caniçada Dam

4.1 Overview of the project

Caniçada Dam is placed on the Cávado river basin, in a region where the river flows over a long and prominent granitic rock mass. It is placed in a reach of the valley with approximate direction of NW-SE, a few kilometres upstream of Parada do Bouro.

Caniçada dam was built in 1955 for hydroelectric power generation. This dam is 76 metres high, has a crest length of 246 metres between left and right abutments and its reservoir has an active capacity of 153 hm^3 and a total capacity of 176 hm^3. It is equipped with a principal spillway composed of 4 stoney gates and a bottom outlet with a maximum discharge of 1700 and 143 $m^3 s^{-1}$, respectively [3, 4].

In 2006, the revision of the Portuguese Dams Security Regulation (Regulamento de Segurança de Barragens) required an improvement of the spillway discharge capacity in order to guarantee the non-exceedance of the normal water level (NWL) of 152.50 m. For this reason, a new spillway was planned to be built on the left abutment of the dam.

The construction work was sequenced such that the spillway construction was performed in-the-dry upstream and the tunnel excavation extended from the downstream outlet and advances toward the reservoir. To do this, temporary L-shaped concrete cofferdam and injections were installed upstream, in order to create a vertical waterproof cut-off wall, with a total length of 134 m.

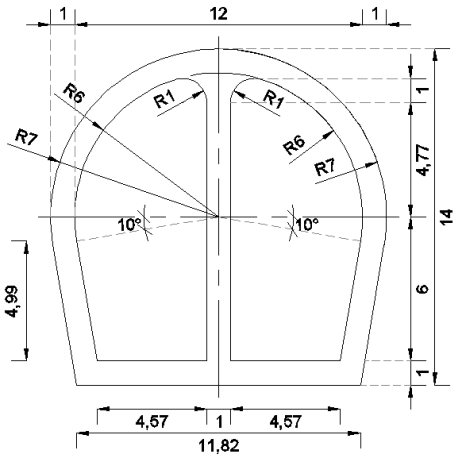

Figure 1: Spillway current section (in metres)

As all construction works downstream were undertaken and completed first, a temporary rock plug was intentionally left near the upstream entrance of the spillway until construction of all tunnel components was completed. The main purpose of this temporary feature was to protect the workers and the project site from potential flooding due to an emergency scenario, such as failure of the temporary cofferdam.

It is a common practice to design this natural rock barrier to have a thickness equal to two to three tunnel diameters. In this case, the rock plug left in place was 27.5 metres thick.

In the scope of this dissertation, this rock plug is assumed to be 16-metre high and 22-metre wide and located between elevations 120.00 and 136.00 m.

4.2 Geotechnical site conditions

The geotechnical site investigation showed that the majority of the spillway was located in a geotechnical zone characterised by a good quality granitic rock mass. Therefore, for the purpose of this dissertation, it shall be a good approximation to consider that the rock mass where the spillway is located is composed of a single material.

The rock mass where the tunnel was excavated is characterised by the following joints set orientations:

J1 - N10°, 40°E

J2 - N330°, 75°NE

J3 - N75°, 90°

J4 - N10°, 90°

J5 - N260°, 75°N

The tunnel is oriented toward direction N84°W.

In order to assess preliminary values for the geotechnical parameters, the RMR classification was performed. For the definition of the ZG1 the following values were assumed:

1. Uniaxial compressive strength of rock material: 2 - 4 MPa
2. Rock Quality Designation (RQD): 50% - 75%
3. Spacing of discontinuities: 200 - 600 mm
4. Condition of discontinuities
   Discontinuity length: $>$ 20 m
   Separation: 0.1 - 1.0 mm
   Roughness: Rough
   Infilling: Hard filling $<$ 5 mm
   Weathering: Slightly weathered
5. Groundwater conditions: Completely dry
6. Orientation of discontinuities: Very favourable

The resulting RMR was 63, corresponding to a class number II described as a "good rock". In order to calculate Hoek-Brown equivalent Mohr-Coulomb parameters, the material constants m_i, m_b and s were estimated through approximation to RMR classification, and the following values were obtained:

m_i = 6.6610 $\quad m_b$ = 1.7858 $\quad s$ = 0.0021

For the estimation of the GSI, the rock mass was assumed to be very blocky and rough, slightly weathered surfaces, and consequently a range of 55-60 was assigned.

In order to use the generalised Hoek-Brown criterion, the values of σ_{ci} and σ'_{3max} of the rock mass had to be assumed. The value of σ_{ci} was based on typical values for granite mass [5]. The value of σ'_{3max} was estimated, and later confirmed, on the numerical simulation performed.

σ_{ci} [MPa] = 50 $\quad \sigma'_{3max}$ [MPa] = 1.5

The resulting values of the Hoek-Brown equivalent Mohr-Coulomb parameters (effective cohesion and internal friction angle) were:

c' [kPa] = 500 $\quad \phi'$ = 40°

Finally, the values of the rock mass unit weight, γ, Young's modulus, E, and Poisson's coefficient, ν, were based on previous works [6]:

γ [kN m^{-3}] = 21

E [MPa] = 400

ν = 0.2

4.3 Object of analysis: emergency scenario

The water-induced pressure on the rock plug following an hypothetical failure of the temporary cofferdam was assessed considering two scenarios: percolation and instant failure. For both scenarios, NWL = 152.50 m will be considered.

Scenario 1 - Percolation

In scenario 1, a process of percolation describes the inward movement of water through the soil, slowly rising the water level inside the temporary cofferdam. This mechanism would generate hydrostatic pressures on the rock plug, as high as the water column inside the temporary cofferdam. The resulting pressure on the rock plug, P, is given by equation eq:eqPSc1, being Π the buoyancy force.

$$P = \frac{\Pi}{s} \tag{6}$$

$$\Pi = \rho \cdot g \cdot h_g \cdot s \tag{7}$$

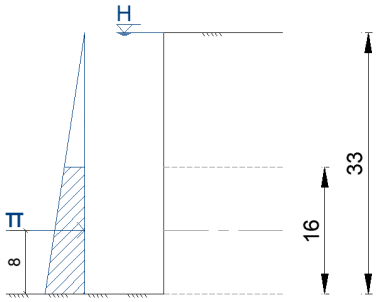

Figure 2: Scenario 1: hydrostatic pressure

The input parameters and results can be found in Table 1.

Table 1: Scenario 1: input parameters and results

Rock plug height [m]	16
Rock plug width [m]	22
Rock plug area (s) [m^2]	352
Water column (H) [m]	33
h_g [m]	25
ρ [kg m^{-3}]	1000
g [m s^{-2}]	9.8
Π [kN]	86240
P [kPa]	245

The value of the resulting pressure is 245 kPa and is constant for the given water column of 33 m.

Scenario 2 - Instant failure

In scenario 2, failure would occur instantly in a portion of the temporary cofferdam. In this case, water would rapidly flow inside the temporary cofferdam and a pressure would be applied to the rock plug instantly. This failure scenario can be solved using an hydraulic

approach through the analysis of broad-crested weirs. The resulting pressure on the rock plug, P, is given by:

$$P = \frac{F}{s} \tag{8}$$

$$F = M + \Pi \tag{9}$$

$$M = \alpha' \cdot \rho \cdot Q \cdot V \tag{10}$$

where Q is the flow rate and V the flow velocity. Fig. 3 illustrates this scenario.

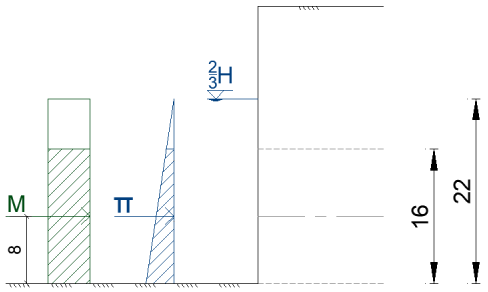

Figure 3: Scenario 2: linear momentum and hydrostatic pressure

The value of P depends on the width of the failure zone, b, because the linear momentum, M, is a function of Q and V, which in turn are functions of b. Thus, the variation of b plays an important role in the analysis of the pressure applied on the rock plug.

The input parameters for this analysis are presented in Table 2.

Table 2: Scenario 2: input parameters

Rock plug height [m]	16
Rock plug width [m]	22
Rock plug area (s) [m^2]	352
Water column ($y_c = \frac{2}{3}H$) [m]	22
h_g [m]	14
ρ [kg m^{-3}]	1000
g [m s^{-2}]	9.8
α'	1

As an example of the results, a pressure of 300, 600 and 900 kPa can be obtained for values of b of approximately 12, 35 and 57 m, respectively.

Comparison between Scenarios 1 and 2

It was concluded that for values of $b < 8$, Scenario 1 governs the maximum pressure applied to the rock plug. If, instead, $b > 8$ then Scenario 2 prescribes the maximum pressure applied.

Although Scenario 2 presents much more significant pressures for large values of b, a scenario of a significant failure of the temporary cofferdam is very unlikely to happen. Therefore, a pressure of 300 kPa was used as a conservative estimate of the hydrostatic pressure.

5 Numerical analysis

5.1 Introduction

Three different simulations were performed.

On the first simulation, a full excavation of the tunnel was carried out in order to validate the model through the comparison between the input initial stress state and the output stress state, and between the expected displacements and the output displacements, given by the software.

On the second simulation, a water-induced pressure was applied on the upstream side of the rock mass and the minimum thickness of the temporary safety rock plug was assessed for an hypothetical emergency scenario.

Lastly, the third simulation consisted of a parametric analysis which intended to evaluate the influence of the pressure, effective cohesion and Young's modulus over the results of the second simulation.

5.2 Model

The geometry adopted for the rock mass and the cross-section on the upstream of the tunnel are illustrated in Fig. 4a and Fig. 4b, respectively.

The initial parameters are presented in Table 3.

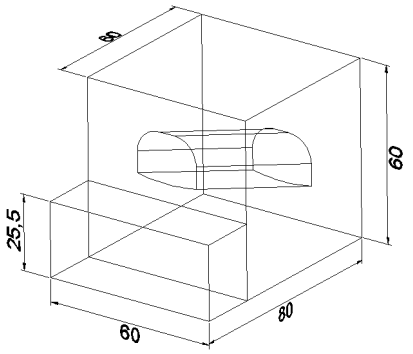

(a) Model geometry

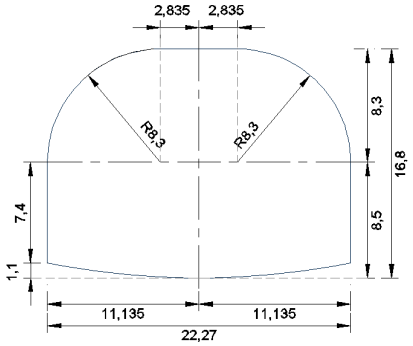

(b) Excavation cross-section near the rock plug

Figure 4: Model dimensions in metres

Step 1, Initial Conditions

In the first step definition, initial stress state and initial loading that contribute to the initial equilibrium were included, as in this step the software checks for equilibrium and iterates, if necessary, to achieve equilibrium.

Table 3: Initial parameters of the rock mass and initial pressure

γ [kPa]	21
ν	0.2
Ψ [°]	0
K_0	0.5
E [MPa]	400
ϕ' [°]	40
c' [kPa]	500
Pressure [kPa]	300

From Step 2 to Step 31 - Excavation process

The next step was to define the excavation sequence as it evolves by deactivating element sets respective to each level of excavation. These deactivation steps are based on the mesh (therefore, elements) adopted for the analysis and for computational limitations the approximate global element size is 2 metres. Consequently, each excavation step will have a length of 2 metres.

Step 32 - Pressure

The final step was to define the pressure in the upstream portal of the tunnel.

Boundary Conditions

The bottom surface was constrained of every displacement and every rotation direction, since it represents the foundation of the rock mass.

All lateral sides facing the limits of the model have rotational constraints in all directions and displacement constraints along axes 1 and 2. The displacement along axis 3 was permitted so that settlements were allowed in the whole model in order to address the geostatic stress state.

The selection of these boundary conditions was preceded by experimental simulations in order to assess the response of the model to the different constraint scenarios.

Predefined stress fields

For this analysis, it was assumed that vertical stress could be reliably obtained from the average density of the overlying rock mass, and the horizontal stresses would be typically assumed as a fraction of the vertical stress, through a coefficient of lateral earth pressure at rest, K_0:

$$\sigma_v = \gamma \cdot h \tag{11}$$

$$\sigma_h = \sigma_v \cdot K_0 \tag{12}$$

Assuming that the rock mass considered is in a location with low tectonic activity [7] and in shallow depth, it was assumed a value of 0.5 for K_0.

Loads

The initial magnitude of the water-induced pressure was defined to be 300 kPa.

Mesh

The model was divided into smaller portions in a partition method. This procedure allows the generated mesh to adjust the many curves and unusual edges of the geometry without refining the mesh. This is a relevant adjustment, since due to computational limitations the mesh should be thought to be the coarsest mesh that can capture the predominant physical behaviour of the rock mass and then refine it where it is expected a high gradient of stresses/strains.

Model validation

Firstly, the defined geostatic stresses should meet the initial stresses verified after equilibrium of the model. It was verified that both stress states were very similar and it was concluded that the inserted initial geostatic stress state was fairly accurate.

Then, it was necessary to verify if displacements associated with the initial stress state were small enough to be neglected. It was expected to have some displacement but it is important that the order of magnitude of these displacements does not influence the displacements of onward analysis. The maximum displacement found in this step was of the order of millimetre or below, which is not relevant for the results, so it can be considered negligible.

Lastly, a displacement verification was performed based on Evert Hoek's estimation of the pattern of deformation in a rock mass surrounding an advancing tunnel, as follows: "Deformation of the rock mass starts about one half a tunnel diameter ahead of the advancing face and reaches its maximum value about one and one half diameters behind the face. At the face position about one third of the total radial closure of the tunnel has already occurred and the tunnel face deforms inwards" as in ([8], p.3). This statement was verified in the model when assessing deformations along the tunnel.

As all verifications were carried out successfully, the model is validated and the simulations could be performed.

5.3 Simulation

In the first place, a simulation was carried out reproducing a full excavation of the rock mass, through the total length of 60 metres, in order to evaluate the behaviour of the rock mass in a full excavation operation.

Afterwards, an analysis was made on an emergency scenario where a water-induced pressure was applied on the upstream face of the rock mass, in order to determine the minimum thickness of the rock plug that withstands this pressure.

Finally, a parametric study assessed how the pressure, cohesion and Young's modulus, some of the focused parameters, influenced the outputs of this study.

5.3.1 Simulation 1, Full excavation

As it can be observed in Fig. 5, the major compressive stresses are located on the lower portions of the sidewalls of the downstream section. This suggests that a special attention should be given to the side-

walls of bottom sections as compressive phenomena may have some impact.

This simulation did not predict any plastic point and, therefore, the model suggests the rock mass will maintain stability.

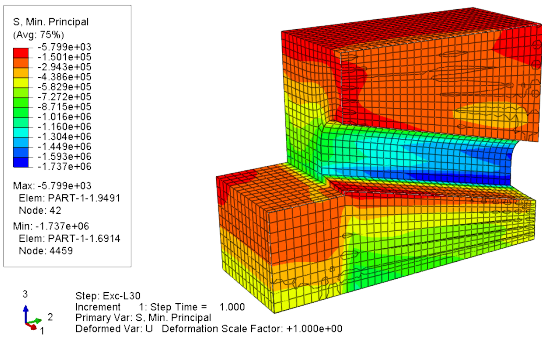

Figure 5: Full excavation: minimum principal stresses

5.3.2 Simulation 2, Emergency scenario

For a 20-metre rock plug, the obtained results confirm that no plasticity occurs when the rock plug is submitted to the designed pressure. These results were expected, as they reflect the traditional approach commonly used in these kind of structures.

It was also verified that no plasticity occurs for a 6-metre rock plug when it is submitted to the designed pressure of 300 kPa.

Lastly, for a 4-metre rock plug, the results show that plastic strain occurs as shown in Fig. 6.

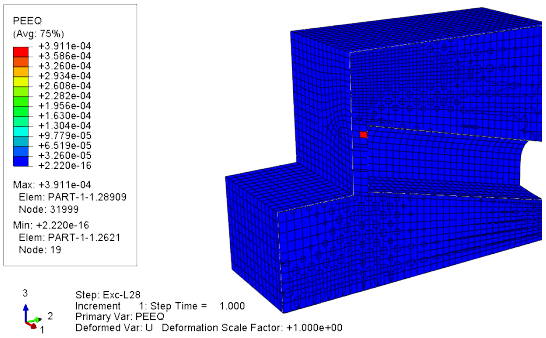

Figure 6: Emergency scenario: equivalent plastic strain at step Exc-L28

According to the results of this analysis, it can be concluded that for a pressure of 300 kPa, a length of at least 6 metres of rock plug can perform a reasonably safe temporary structure for this kind of works. Thus, this analysis demonstrates that for this kind of features the conventional method can overdesign a temporary structure that will, consequently, increase the expenditure of works.

5.3.3 Simulation 3, Parametric study

A parametric study was performed in order to study the influence of some parameters used in the simulation. The chosen parameters were the pressure (P), cohesion (c') and Young's modulus (E).

Pressure (P)

When the pressure applied to the rock plug is 300 kPa, the model shows plastic points for thicknesses up to 4 metres, as previously shown in Fig. 6.

If the pressure considered would be 600 kPa, the model displays plastic points for thicknesses up to 6 metres, as illustrated in Fig. 7.

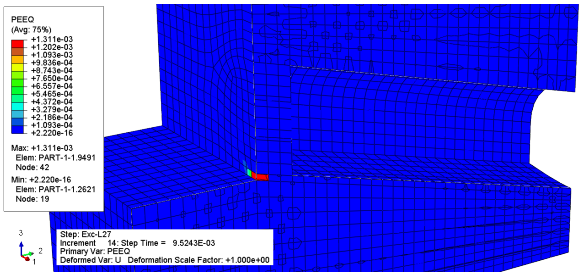

Figure 7: Parametric analysis: equivalent plastic strain at step Exc-L27 for P=600 kPa

When the pressure applied is 900 kPa, the model exhibits plastic points for thicknesses up to 10 metres, as illustrated in Fig. 8. For thicknesses starting at 12 metres, no yielding occurs.

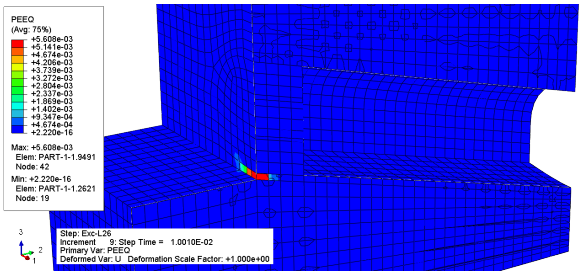

Figure 8: Parametric analysis: equivalent plastic strain at step Exc-L26 for P=900 kPa

From the results above, it can be concluded that as the pressure applied on the mass rock increases, the necessary thickness of the rock plug must be larger to endure the load without compromising the rock mass stability.

Cohesion (c')

Considering a thickness of 6 metres for the rock plug, no yielding occurs for a cohesion value of 500 kPa, as previously shown in Fig. 6.

However, if cohesion value would be of 400 kPa, Fig. 9 shows that plastic points would occur on the sidewalls of bottom sections.

If a value of 300 kPa would be considered for cohesion, several plastic points would occur on the sidewalls of the majority of the excavation (Fig. 10).

From the results above, it can be concluded that as the cohesion of the mass rock decreases, the rock strength decreases significantly and failure is more likely to occur.

Young's modulus (E)

Considering a thickness of 6 metres for the rock plug, Fig. 11 illustrates that for E = 400 MPa the maximum displacement is of 4.728e-02 m.

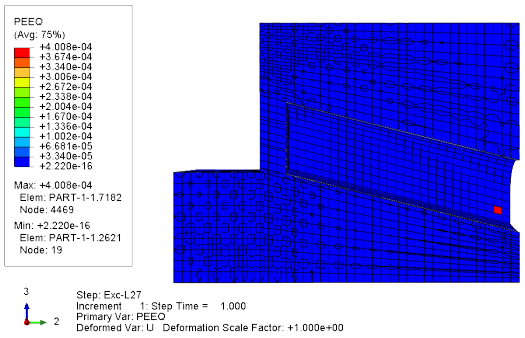

Figure 9: Parametric analysis: equivalent plastic strain at step Exc-L27 for c'=400 kPa

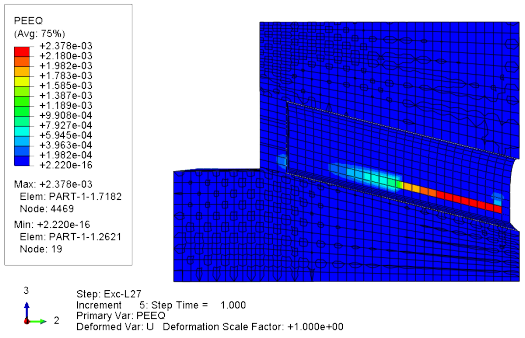

Figure 10: Parametric analysis: equivalent plastic strain at step Exc-L27 for c'=300 kPa

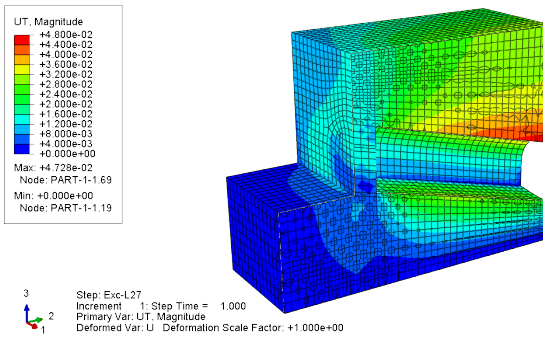

Figure 11: Parametric analysis: displacements at step Exc-L27 for E=400 kPa

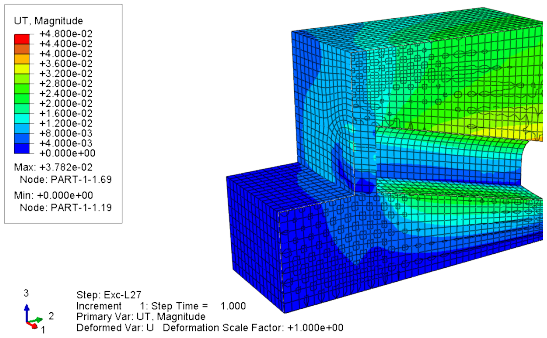

Figure 12: Parametric analysis: displacements at step Exc-L27 for E=500 kPa

If a value of 500 MPa would be assumed for Young's modulus, the maximum displacement would be 3.782e-02 m, as illustrated in Fig. 12.

For a value of Young's modulus of 600 MPa, the maximum displacement would be 3.152e-02 m, as illustrated in Fig. 13.

From these results it can be concluded that as E increases, the values of the maximum displacements decrease. This was an expected conclusion since the stiffness of a material is inversely proportional to its deformation and, therefore, the herein maximum displacements are controlled by the Young's modulus assigned.

5.4 Discussion of results and concluding remarks

The first simulation intended to evaluate the stability of the rock mass when submitted to a full unsupported excavation operation, without considering any water-pressure effects. The results of this operation showed that, although some significant displacements would occur, the stability of the rock mass was verified.

On the second simulation, the results showed that, for the rock mass considered, a rock plug with a thickness of 6 metres would endure the hypothetical emergency scenario considered. This result suggests that the traditional empirical method used in this project for the estimation of the thickness of this temporary structure is very conservative.

Lastly, the third simulation concluded that the input parameters have a critical role in the definition of the model response. For instance, for the maximum pressure considered, 900 kPa, equivalent to a significant failure of the temporary cofferdam in the upstream zone, the minimum thickness necessary to endure this load is 12 metres, less than half of the adopted dimension (27.5 m).

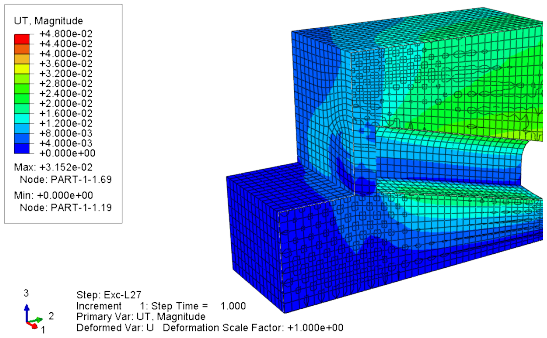

Figure 13: Parametric analysis: displacements at step Exc-L27 for E=600 kPa

6 Analysis of structural features

In shallow underground excavations in jointed rock masses, some of the most common types of failure are those ruled by faults, joints, shear zones and bedding planes. The presence and intersection of these structural features results in partitioning of the rock mass into discrete but interlocked fractions which may become unstable as the excavation works advance.

A stability analysis of the structural features was carried out using *RocScience Unwedge*, a software for 3D

stability analysis of underground excavations in rock masses containing intersecting structural discontinuities.

In this software discontinuities are assumed to be persistent, ubiquitous and their surfaces are assumed to be perfectly planar, and as wedges are tetrahedral and defined by three intersecting discontinuities, *Unwedge* analyses a maximum of three joint planes at one time.

6.1 Stability analysis prior reinforcement

For this analysis, the factor of safety was considered to be the most critical aspect and the wedges herein presented are sorted by this criterion.

Table 4: Input parameters: tunnel, rock and factor of safety

Tunnel axis orientation	
Trend	284
Plunge	5
Design factor of safety	2
Rock unit weight [MN m^{-3}]	0.021

Table 5: Input parameters: joints (average values)

Joints - Orientations		
Joint	Dip	Dip Direction
F1	50	190
F2	15	150
F3	0	255
F4	0	190
F5	15	80
Joints - Shear strength properties		
Model		Mohr-Coulomb
ϕ' [°]		40
c' [kPa]		0
Tensile strength [MPa]		0
Elastic behaviour assumed		

The evaluation of potential wedge sliding is represented in Fig. 14, showing the geometry and location of five wedges, numbered 3, 4, 5, 6, 7.

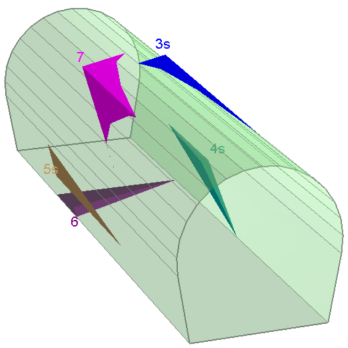

Figure 14: Identification of potential wedges

The analysis showed that wedge number 4 was unstable, with a factor of safety of 0.7, which means that any sort of mitigation measure shall be adopted.

6.2 Stability analysis after reinforcement

This case-study tunnel's support comprises the installation of an initial support based on steel fiber-reinforced shotcrete with swellex rockbolts. This was the reinforcement solution employed in this simulation, with the parameters in Table 6.

Table 6: Input parameters: perimeter support

Perimeter support - Shotcrete properties	
Shear strength [MPa]	0.7
Unit weight [MN m^{-3}]	0.025
Thickness [cm]	6
Perimeter support - Bolt properties	
Type	Swellex
Tensile capacity [MN]	0.14
Bond strength [MN/m]	0.15
Perimeter support - Bolt pattern on perimeter	
Length [m]	4
Pattern spacing in plane [m]	2.5
Pattern spacing out of plane [m]	2.5

Fig. 15 displays the reinforcement solution on the tunnel's profile.

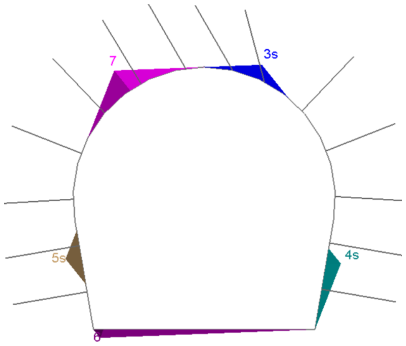

Figure 15: Installation of reinforcement (shotcrete and rockbolts): front view

With the installation of the support, it was concluded that all wedges were stable. Wedge number 4 increased its factor of safety to 33.2.

6.3 Discussion of results

It was verified that the support solution designed for this tunnel is stable in what wedge instabilities do concern, for the given joints set. The results presented show that the factor of safety for every wedge considered increased significantly after the installation of the shotcrete and the rockbolts.

7 Conclusions and future work

It was found that for a pressure of 300 kPa, assumed as the most realistic failure scenario, the minimum thickness of the rock plug was 6 metres. When changing this pressure from 300 to 900 kPa, the necessary thickness has increased, as expected, since a larger amount of rock mass is necessary to withstand

larger loads. It should be noted that even for the worst-scenario considered, 900 kPa, the minimum thickness was 12 metres. This corresponds to less than 50% of the adopted dimension for this structure, suggesting that the allocation of resources could have been reduced.

When reducing the effective cohesion from 500 to 300 kPa, it was observed that failure occurred on the sidewalls of the bottom part of the tunnel. This might have happened due to the range of stresses in the rock mass and the geometry defined for the tunnel section.

Finally, it was noted that Young's modulus had no relevant effect on the thickness of the rock plug, although displacements are highly related to this parameter, since displacements decrease as the Young's modulus increases.

The results obtained show some evidence that the traditional method of considering two or three tunnel diameters for this thickness for similar geological scenarios might be too conservative and results in a time-consuming and less cost-effective project.

Regarding failure mechanisms related to discontinuities, it is worthwhile to emphasise the importance of an adequate and continuous geological site investigation for a stability analysis to take place as part of the design project. Prior to any excavation works, careful and attentive geotechnical site investigations can provide useful information regarding any expected wedge instability. However, a continuous study of these structural features encountered in the excavation process and the identification and visualisation of potentially unstable blocks and wedges is of foremost relevance.

Further investigation and other possible developments to the analyses discussed in this work could be:

- A more exhaustive numerical strategy considering, for instance, the primary and/or final support;
- A study on how heterogeneity of rocks can be implemented in a numerical model, namely by assessing the effects of variable discretization in simulations such as the one performed;
- The consideration of other approaches for the estimation of rock mass parameters, initial stress states and stress and failure criteria.

References

[1] Brady, B. H. G., Brown, E. T., *Rock Mechanics for Underground Mining*. Springer Science, 3 ed., 2005.

[2] Ceballos, F., Olalla, C., Jimenez, R., "Relationship between RMRb and GSI based on in situ data," in *EUROCK Vigo 2014, ISRM European rock mechanics symposium*, (Vigo), May 2014.

[3] EDP Gestão da Produção de Energia S. A., "Declaração Ambiental Aproveitamentos Hidroeléctricos da EDP Produção." http://www.a-nossa-energia.edp.pt/pdf/desempenho_ambiental/Declaracao_Ambiental_Aproveitamentos_Hidroeletricos_2015.pdf (access date: May 2017), 2015.

[4] Comissão Nacional Portuguesa das Grandes Barragens, "Caniçada Dam." http://cnpgb.apambiente.pt/gr_barragens/gbingles/FichasIng/CanicadafichaIng.htm (access date: May 2017).

[5] Tavares, A., "Revestimento de Túneis Hidráulicos em Betão Projetado," Master's thesis, Instituto Superior Técnico, Universidade de Lisboa, 2014.

[6] Calatróia, J., "Execução de ensecadeiras com recurso a cortinas de injeções e de colunas de Jet Grouting," Master's thesis, Instituto Superior Técnico, Universidade de Lisboa, 2016.

[7] World Stress Map, "Stress Map of the Mediterranean and Central Europe 2016." http://escidoc.gfz-potsdam.de/ir/item/escidoc:1809897/components/component/escidoc:1868888/content (access date: May 2017), 2016.

[8] Hoek, E., "Tunnel support in weak rock," in *Symposium of Sedimentary Rock Engineering*, (Taipei), November 1998.

[9] Hoek, E., Kaiser, P. K., Bawden, W. F., *Support of Underground Excavations in Hard Rock*. New York: Taylor & Francis, 1995.

[10] Sjölberg, J., "Estimating Rock Mass Strength Using the Hoek-Brown Failure Criterion and Rock Mass Classification - A Review and Application to the Aznalcollar Open Pit," tech. rep., Division of Rock Mechanics, Luleå University of Technology, 1997.

[11] White, F. M., *Fluid Mechanics*. New York: McGraw-Hill, 4 ed., 2003.

[12] Hoek, E., Carranza-Torres, C., Corkum, B., "Hoek-Brown Failure Criterion – 2002 Edition," in *Proc. NARMS-TAC Conference*, (Toronto), pp. 267–273, 2002.

[13] Álvarez, D. L., "Limitations of the Ground Reaction Curve Concept for Shallow Tunnels Under Anisotropic In-situ Stress Conditions," Master's thesis, KTH Royal Institute of Technology, 2012.

[14] Hoek, E., "Practical Rock Engineering." https://www.rocscience.com/documents/hoek/corner/Practical-Rock-Engineering-Full-Text.pdf (access date: April 2017), 2007.

[15] Afaplan, "Caniçada Dam." http://afaplan.com/projecto?id=28 (access date: May 2017).

[16] Hoek, E., Brown, E. T., "Practical estimates of rock mass strength," *International Journal of Rock Mechanics and Mining Sciences*, vol. 34, pp. 1165–1186, December 1997.

[17] Rock Mass - Geology applied in rock construction, "Short on the RMR (Rock Mass Rating) system." http://http://www.rockmass.net/files/short_on_RMR-system.pdf (access date: May 2017).

[18] Hoek, E., Brown, E. T., "The Hoek-Brown Failure Criterion - a 1988 Update," in *15th Canadian Rock Mechanics Symposium*, pp. 31–38, 1988.

[19] Bieniawski, Z. T., *Engineering Rock Mass Classifications*. Wiley-Interscience, 1989.

[20] Dassault Systèmes, "SIMULIA User Assistance 2017." http://help.3ds.com/2017/English/DSSIMULIA_Established/SIMULIA_Established_FrontmatterMap/SIMULIA_EstablishedDocSearchOnline.htm?ProductType=DS&ProductName=DSSIMULIA_Established&ContextScope=all (access date: March 2017), 2017. Software Abaqus/CAE.

[21] Hoek, E., "Rock Mechanics - an introduction for the practical engineer (Parts I, II and III)," *Mining Magazine*, April, June and July 1966.

[22] Palmström, A., *RMI - A Rock Mass Characterization System For Rock Engineering Purposes*. PhD thesis, Oslo University, 1995.

[23] Brandão, L., "Modelação Numérica 3D de Escoamentos em Descarregadores de Cheia - Aplicação ao descarregador de cheias complementar do aproveitamento hidroelétrico da Caniçada," Master's thesis, Faculdade de Engenharia, Universidade do Porto, 2015.

[24] Real, P., "Coordenação de Segurança em Obra – Metodologia, Técnicas e Ferramentas," Master's thesis, Escola de Engenharia, Universidade do Minho, 2015.

[25] ITA Working Group on General Approaches to the Design of Tunnels, "Guidelines for the Design of Tunnels," *Tunnelling and Underground Space Technology*, vol. 3, pp. 237–249, 1988.

[26] Santos, V., *Gestão de Risco Geotécnico na Construção de Túneis em Maciços Rochosos*. PhD thesis, Faculdade de Ciências e Tecnologia, Universidade Nova de Lisboa, 2016.